TÜBİTAK

Turk J Elec Eng & Comp Sci,
Vol.17, No.1, 2009, © TÜBİTAK
doi:10.3906/elk-0801-1

Electronic Differential with Direct Torque Fuzzy Control for Vehicle Propulsion System

Kada HARTANI[1], **Mohamed BOURAHLA**[2],
Yahia MILOUD[1], **Mohamed SEKOUR**[1]
[1] *Electrotechnic Department, University center of Saida, Bp 138 En-Nasr, 20000 Saida-ALGERIA*
e-mail: kada_hartani@yahoo, miloudyahiadz@yahoo.fr, msekour@yahoo.fr
[2] *University of Sciences and Technology of Oran BP 1505El Menouar 31000, Oran-ALGERIA*
e-mail: bourah3@yahoo.fr

Abstract

We model an electronic differential that will offer the best vehicle stability on a curved road. The proposed traction system consists of two permanent magnet synchronous (PMS) machines that ensure the drive of two back-driving wheels. The contribution of each wheel to the advance of the vehicle is represented by an element conveying the accumulation of mechanical coupling. The proposed control structure is based on the direct torque fuzzy control for each wheel-motor. Different simulations have been carried out: vehicle driven ons straight road, vehicle driven on straight road with slope, and vehicle driven over a road curved left and right. The simulation results show good vehicle stability on a curved road.

Key Words: *Electric vehicle, electronic differential, direct fuzzy torque control, permanent magnet synchronous motor.*

1. Introduction

Traction drive used in electric vehicles can be divided into two categories: (i) single-drive system and (ii) multi-drive systems. With multi-drive systems the motor controllers must additionally be configured to provide an electronic differential effect i.e. they must also perform a similar function as their mechanical differential counterpart. Thus the electronic differential must take account of the speed difference between the two wheels when cornering.

The proposed traction system consists of two permanent magnet synchronous machines (PMSM) that ensure the drive of the two back-driving wheels. Such systems are known as multi-machine multi-converter systems (MMS) [1] and are recognized via the coupling system type: either an electric nature, or a magnetic and/or mechanical coupling used in several electric machines propelling the vehicle. The proposed control structure [2], called *independent machines for speed control*, is an electronic differential method based on direct torque fuzzy control (DTFC).

This direct torque fuzzy control uses the stator flux amplitude and measurement of electromagnetic torque errors via two fuzzy logic controllers to generate a voltage space vector (reference voltage) from both the amplitude and angle of its components; and in turn is used by space vector modulation to provide the inverter switching states. The methods of Mamdani and Sugeno provide the fuzzy reasoning algorithms in the two fuzzy logic controllers.

The main goal of using a DTFC algorithm for PMSM drives is to overcome some of the drawbacks of the conventional DTC [3]. However, this greatly reduces torque ripple and the fast response and robustness merits of the classical DTC [3–4] are entirely preserved by eliminating hysteresis regulators of flux and torque.

In order to characterise the electronic differential system for an electric vehicle driven by two permanent magnet synchronous motors attached to the rear wheel using direct torque fuzzy control, differents simulations have been carried out: simulating the vehicle driven vehicle on a straight road, a straight road with slope, and driven over a road curved right and left.

2. Traction System Proposed

The usual configuration of electrical or non-electrical vehicles involves only one traction motor driving two wheels, using a differential gear, as illustrated in Figure 1(a) [5]. In this work, we adopt a structure with two independent wheel drives. A rear-driven, two-motor configuration controlled independently using an electronic differential is shown in Figure 1(b). This configuration offers full control of the torque applied to each of the wheels and an increased capacity for regenerative braking.

The motor wheel allows packaging flexibility by eliminating the central drive motor and the associated transmission and driveline components in vehicles, including the transmission, differential, universal joints and drive shaft.

A major benefit of the in-wheel motor (Figure 2) is that it enables drive torque and braking force to be regulated with high precision on an individual wheel basis in both two wheel drive systems without requiring transmissions, drive shafts, differential gears or other complex and heavy components.

In this work, we consider a two-wheel driven vehicle with independent drive on each wheel, as shown Figure 1(b). Such a vehicle may present advantages such as increasing the vehicle power with a better weight distribution and no power loss in the differential gear, and the possibility of controlling the acceleration of each wheel individually for better stability during difficult or dangerous situations.

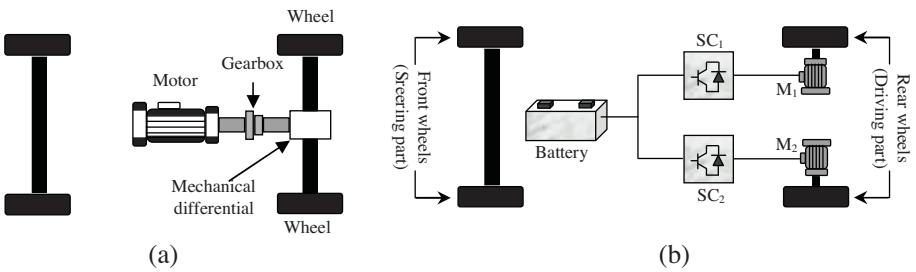

Figure 1. Vehicle structure with (a) one central motor; (b) two independent rear wheels.

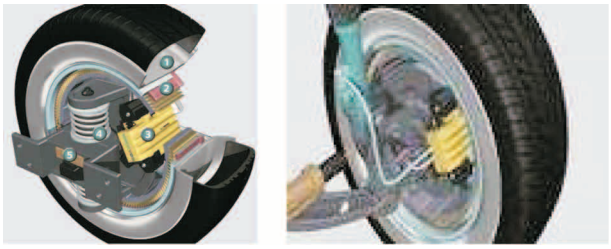

Figure 2. Drawing showing in-wheel motor.

Such a two-wheel-independently-driven system is a multi-machine system, and such systems are characterized by the coupling of different electromechanical conversion systems. The system is diagrammed in Figure 1, and for the present study is characterized by only one coupling. The topology is illustrated in Figure 3. In order to realize the electronic differential, the independent-machine control structure is applied to the traction system of two driving wheels by a speed control. See Figure 4 for the control system topology.

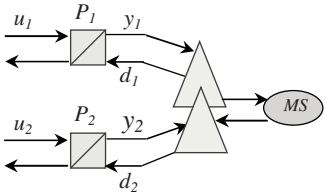

Figure 3. Topology of the two-wheel-independently-driven system discussed in the present study.

2.1. Independent machine control structure

This structure presently explored is composed of two machines controlled independently as two single machine structures. Each machine can be imposed to a different speed (which, in the present case, $\Omega_{\mathrm{l}_{\mathrm{Rref}}} \neq \Omega_{\mathrm{r}_{\mathrm{Rref}}}$ for the left and right drives) using static converters. These machines are uncoupled through the control structure and reject all disturbances like single machine control [6]. The principle of this control is illustrated in Figure 4.

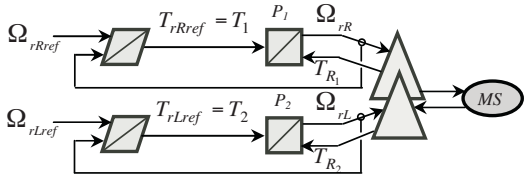

Figure 4. Control structure for the independent-machine structure used in the present study.

3. Global System Modelling

The proposed electric vehicle drive system has two PMS motors for the rear wheel drives, as illustrated in Figure 5. With multi-drive systems, the motor controllers must additionally be configured to provide an electronic differential effect, i.e. they must also perform a similar function as their mechanical differential counterpart.

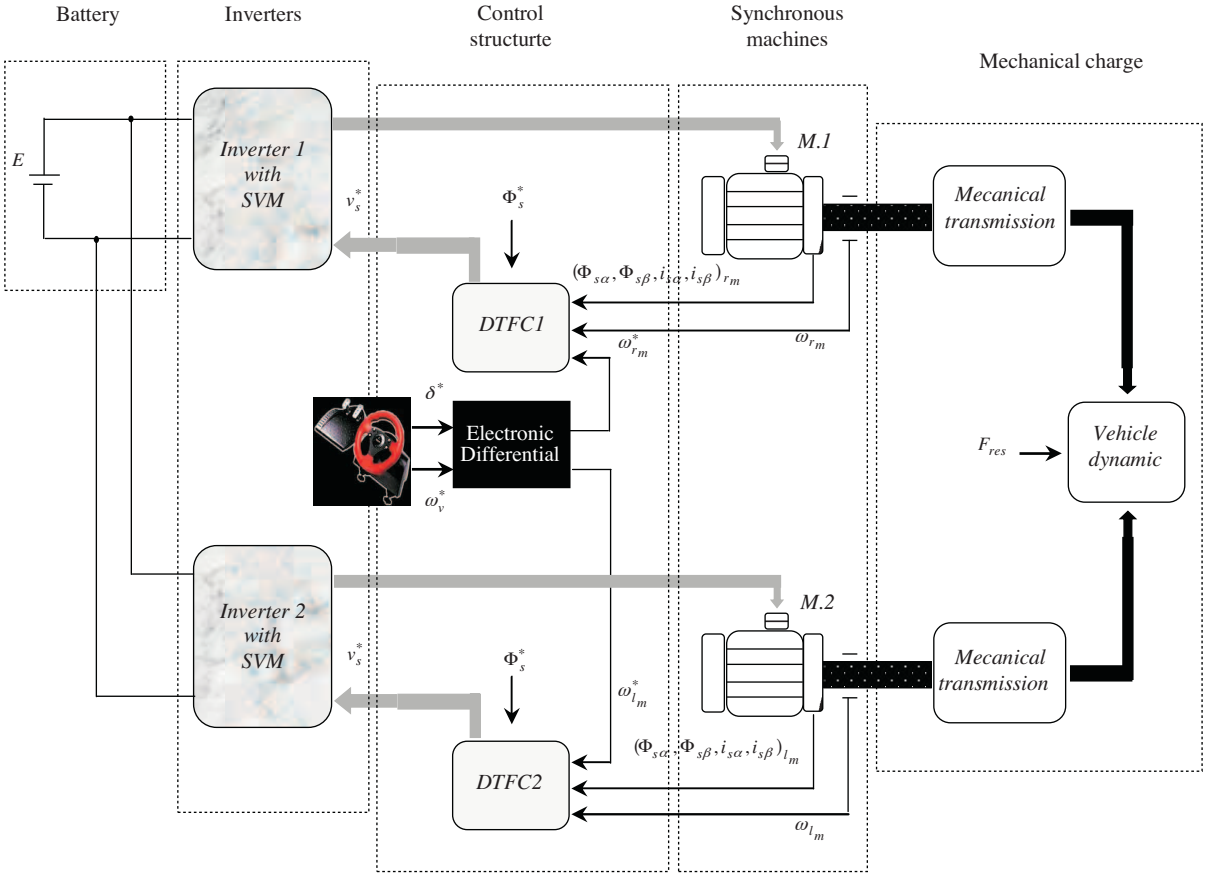

Figure 5. Basic block diagram of the system for controlling the drive wheels.

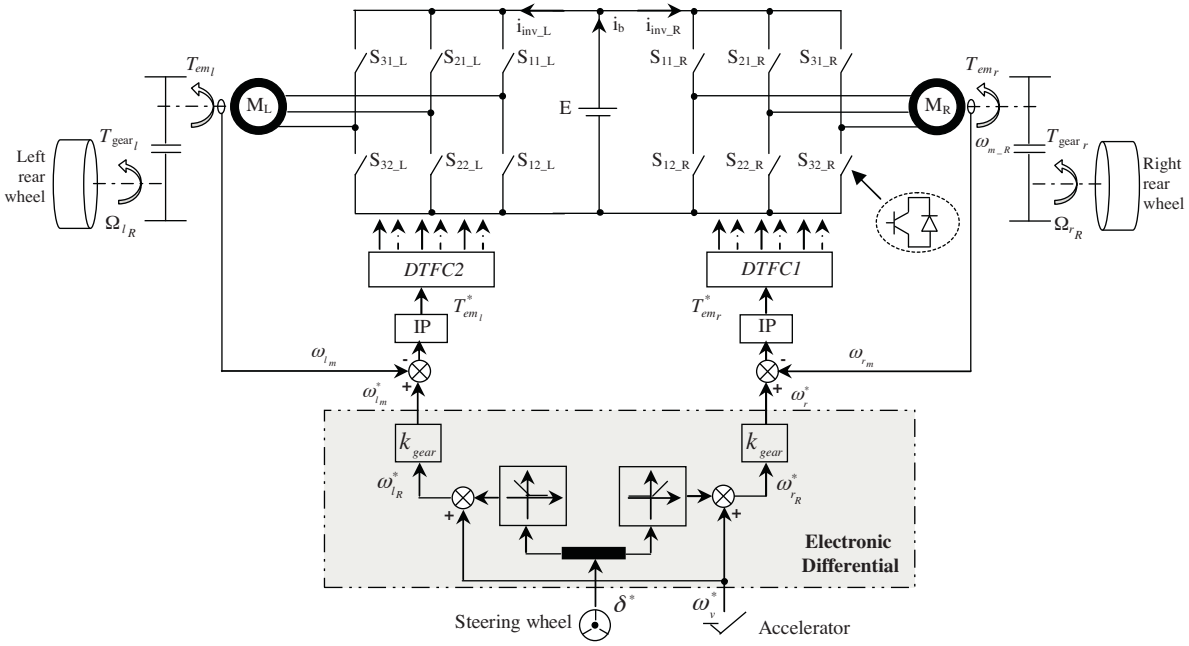

Figure 6. Components of the proposed control system.

Thus, the electronic differential must take account of the speed difference between the two wheels when cornering. The system uses the vehicle speed and steering angle as input parameters and calculates the required inner and outer wheel speeds where the two rear wheels are controlled independently by two PMS motors. Figure 6 shows the proposed system control for the electronic differential based on DTFC control.

3.1. Modelling the electronic differential

The considered propulsion system architecture permits one to develop an electronic differential to assure that, over a straight trajectory the two wheel drives roll exactly at the same velocity; and in a curve trajectory the difference between the two wheel velocities assure the vehicle trajectory over the curve. See Figure 7. Since the two rear wheels are directly driven by two separate motors, the speed of the wheel at the outer position of the curve will need to be greater than the speed of the inner wheel during curved steering (and vice versa); this helps the tyres from loosing traction in turns. Figure 7(b) shows the vehicle structure describing a curve, where L_w represents the wheelbase, δ the steering angle, d_w the distance between the wheels of the same axle and ω_L and ω_R the angular speeds of the left and right wheel drives, respectively.

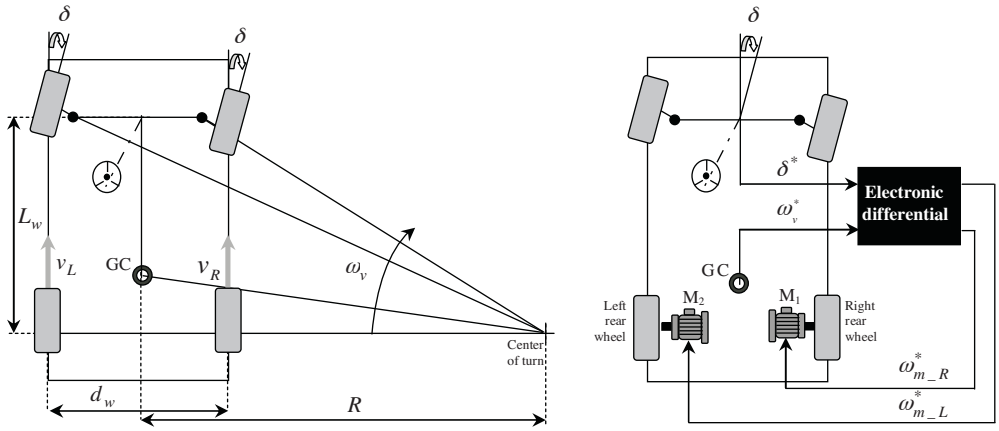

(a) (b)

Figure 7. (a) Structure of electronic differential. (b) Design model for vehicle structure driven in a curve.

The linear speed of each wheel drive is expressed as a function of the vehicle speed and the radius of curve:

$$v_L = \omega_v \left(R + \frac{d_w}{2} \right), \tag{1}$$

$$v_R = \omega_v \left(R - \frac{d_w}{2} \right). \tag{2}$$

The curve radius is related to the wheelbase and steering angle:

$$R = \frac{L_w}{\tan \delta}. \tag{3}$$

Substituting (3) into equations (1) and (2), we obtain the angular speed in each wheel drive:

$$\omega_{r_L} = \frac{L_w + \frac{1}{2} d_w \tan \delta}{L_w} \omega_v \tag{4}$$

$$\omega_{\mathrm{r}_R} = \frac{L_w - \frac{1}{2} d_w \tan\delta}{L_w} \omega_v. \tag{5}$$

The difference between the angular speeds of the wheel drives is expressed by the relation

$$\Delta\omega = \omega_{l_R} - \omega_{r_R} = \frac{d_\omega \cdot \tan\delta}{L_\omega} \omega_v. \tag{6}$$

Numeric sign of the steering angle signal indicates the curve direction:

$$\begin{array}{l} \delta > 0 \Rightarrow \text{Turn right} \\ \delta = 0 \Rightarrow \text{Straight ahead} \\ \delta < 0 \Rightarrow \text{Turn left.} \end{array} \tag{7}$$

When the vehicle begins a curve, the driver imposes a steering angle to the wheels. The electronic differential however acts immediately on the two motors reducing the speed of the inner wheel and increases the speed of the outer wheel; see Figure 8. The driving wheel angular speeds are

$$\omega^*_{l_R} = \omega_v + \frac{\Delta\omega}{2} \tag{8}$$

$$\omega^*_{r_R} = \omega_v - \frac{\Delta\omega}{2}. \tag{9}$$

The speed references of the two motors are:

$$\omega^*_{l_m} = k_{\mathrm{gear}} \omega^*_{l_R} \tag{10}$$

$$\omega^*_{r_m} = k_{\mathrm{gear}} \omega^*_{r_R}, \tag{11}$$

where k_{gear} is the gearbox ratio.

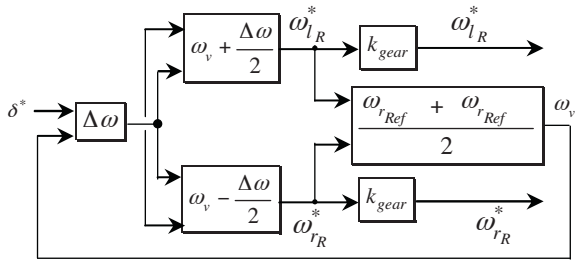

Figure 8. Block diagram show use of the electronic differential.

3.2. Traction motor model

The PMSM model can be described in the stator reference frame via the system of equations

$$\begin{cases} \frac{di_{s\alpha}}{dt} = -\frac{R_s}{L_s} i_{s\alpha} + \frac{\Phi_f}{L_s} \omega_m \sin\theta + \frac{1}{L_s} v_{s\alpha} \\ \frac{di_{s\beta}}{dt} = -\frac{R_s}{L_s} i_{s\beta} - \frac{\Phi_f}{L_s} \omega_m \cos\theta + \frac{1}{L_s} v_{s\beta} \\ \frac{d\omega_m}{dt} = -\frac{f}{J} \omega_m + \frac{p}{J} \left(T_{em} - T_r\right) . \end{cases} \tag{12}$$

Electromagnetic torque equation is expressed as

$$T_{\mathrm{em}} = \frac{3}{2} p \Phi_f \left(-i_{s\alpha} \sin\theta + i_{s\beta} \cos\theta\right). \tag{13}$$

3.3. Inverter model

In this electric traction system, we use a voltage inverter to obtain three balanced phases of alternating current with variable frequency. The voltages generated by the inverter are given as follows:

$$\begin{bmatrix} v_a \\ v_b \\ v_c \end{bmatrix} = \frac{E}{3} \begin{bmatrix} 2 & -1 & -1 \\ -1 & 2 & -1 \\ -1 & -1 & 2 \end{bmatrix} \begin{bmatrix} S_a \\ S_b \\ S_c \end{bmatrix}. \tag{14}$$

3.4. Energy source

The source of energy is generally a Lithium-Ion battery system. Lithium-Ion battery technology offers advantages of specific energy, specific power, and life over other types of rechargeable batteries [8–11].

3.5. Vehicle dynamic

The total resistive force is defined as [12]

$$F_{\text{res}} = F_{\text{roll}} + F_{\text{aero}} + F_{\text{slope}} \tag{15}$$

and

$$F_{\text{roll}} = \mu M g \tag{16}$$

$$F_{\text{aero}} = \frac{1}{2}\rho C_x S v_h^2 \tag{17}$$

$$F_{\text{slope}} = Mg \cdot \sin\alpha \tag{18}$$

where F_{roll} is the rolling resistance, F_{aero} is the aerodynamic drag force and F_{slope} is the slope resistance.

4. PMSM DTFC System

4.1. Principe of DTFC

Fuzzy logic method is used in this study to improve the steady state performance of a conventional DTC system. Figure 9 schematically shows a direct torque fuzzy control in which the fuzzy controllers replaces the flux linkage and torque hysteresis controllers and the switching table normally used in a conventional DTC system [13–15].

Table 1. FLC rules.

$\frac{\tilde{e}_c \rightarrow}{\tilde{e}_\Phi \downarrow}$	NG	NM	NP	EZ	PP	PM	PG
NG	PG	PM	PP	PP	PP	PM	PG
NM	PG	PM	PP	PP	PP	PM	PG
NP	PG	PM	PP	EZ	PP	PM	PG
EZ	PG	PM	PP	EZ	PP	PM	PG
PP	PG	PM	PP	EZ	PP	PM	PG
PM	PG	PM	PP	PP	PP	PM	PG
PG	PG	PM	PP	PP	PP	PM	PG

Table 2. Reference voltage increment angle.

$\varepsilon^n_{\Phi_s}$	P			Z			N		
ε^n_c	P	Z	N	P	Z	N	P	Z	N
δ	$\frac{\pi}{4}$	0	$\frac{-\pi}{4}$	$\frac{\pi}{2}$	$\frac{\pi}{2}$	$\frac{-\pi}{2}$	$\frac{3\pi}{2}$	π	$\frac{-3\pi}{4}$

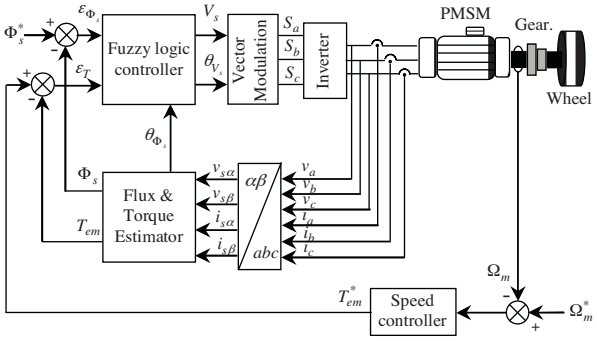

Figure 9. Schematic showing the structure of the Direct torque fuzzy control (DTFC) scheme used in the present study. The fuzzy controllers replace the flux linkage and torque hysteresis controllers and the switching table used in a conventional DTC system.

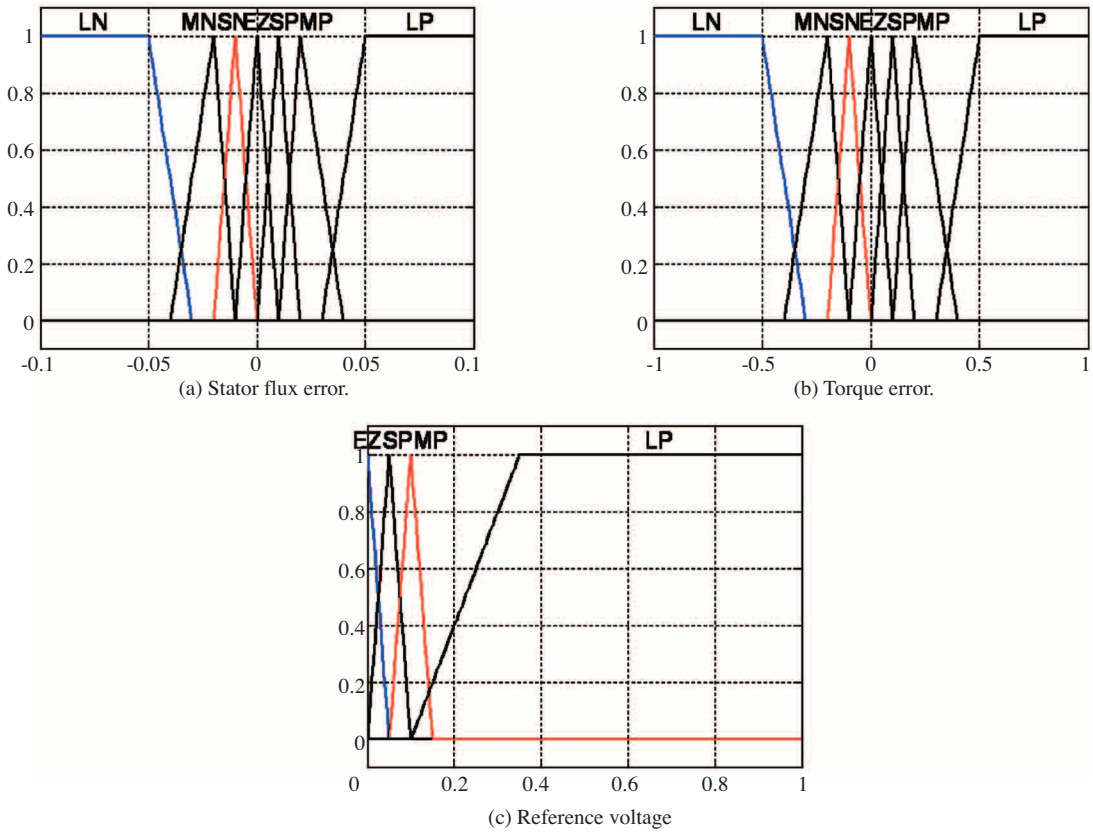

Figure 10. Membership functions for Fuzzy Logic Controller 1 (FLC1).

The proposed DTFC scheme uses the stator flux amplitude and the electromagnetic torque errors, processed through two fuzzy logic controllers to generate a voltage space vector (reference voltage) by acting on both the amplitude and the angle of its components, which is used via space vector modulation to generate the inverter switching states. In Figure 10, the errors of the stator flux amplitude and the torque are selected as the inputs; the reference voltage amplitude is the output of fuzzy logic controller 1 (FLC1); the increment angle is the output of fuzzy logic controller 2 (FLC2). The increment angle is added to the angle of the stator flux vector and the results are delivered to the space vector modulation which calculates the switching states S_a, S_b and S_c. The methods of Mamdani's and Sugeno are employed in the fuzzy reasoning algorithms used by FLC1 and FLC2, respectively. Figure 11 and Figure 12 depict the membership functions for both fuzzy logic controllers FLC1 and FLC2, respectively.

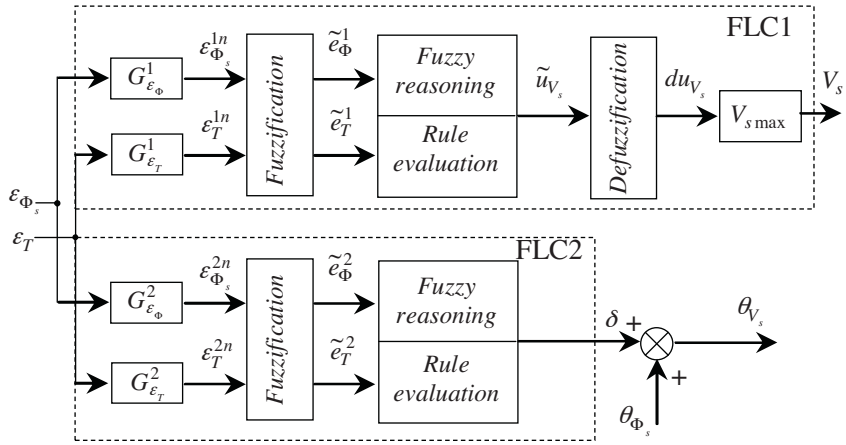

Figure 11. Fuzzy logic controller structure.

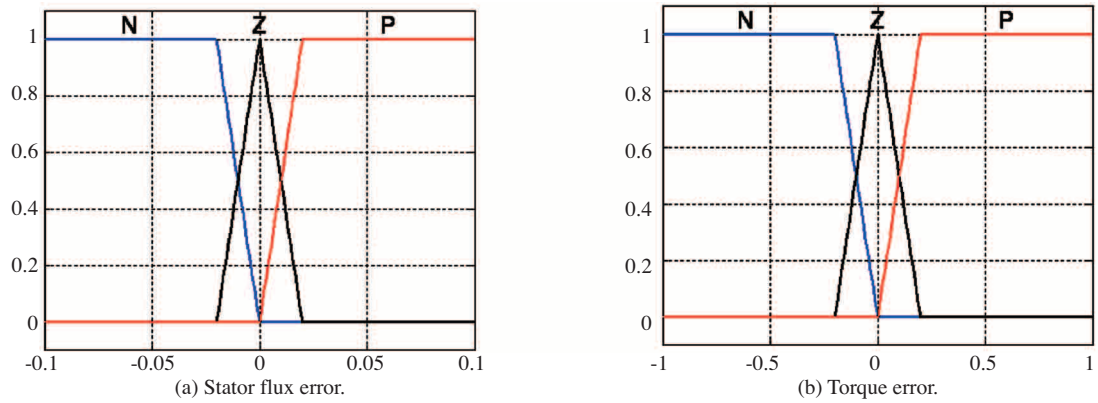

(a) Stator flux error. (b) Torque error.

Figure 12. Membership functions for Fuzzy Logic Controller 2 (FLC2).

4.2. Conventional speed controllers

As a comparison, both proportional-integrator (PI) controllers and integrator-proportional (IP) controllers, with anti-windup strategy [16, 17] (schematized in Figure 13 and Figure 14), are used in the proposed DTFC scheme to obtain the reference torque T^*_{em}.

It is clear that from Figure 15, the IP controller performs better then the PI controller as the overshoot speed and time response are reduced.

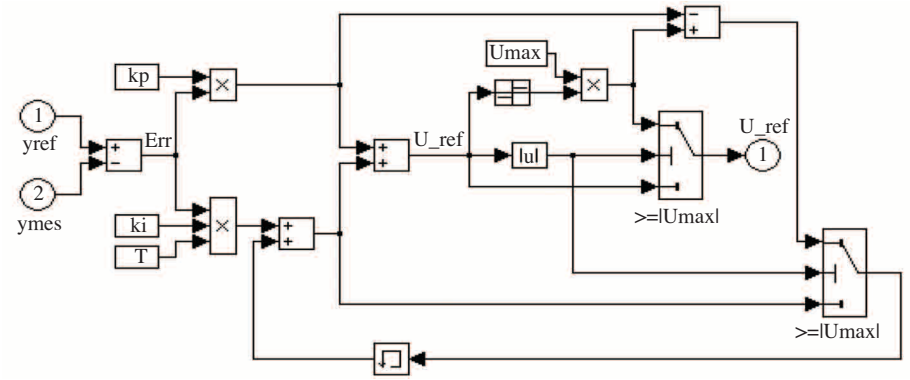

Figure 13. Simulink model of corrector PI with *anti-windup* strategy.

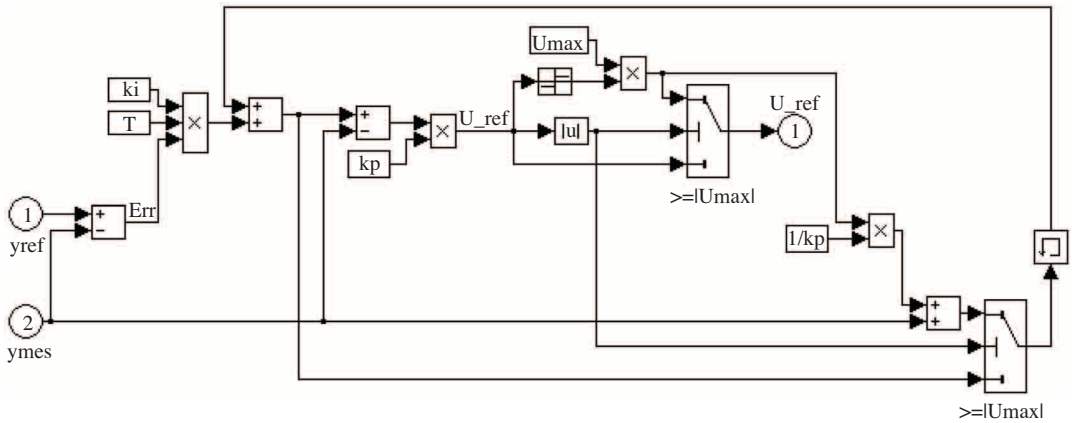

Figure 14. Simulink model of corrector IP with *anti-windup* strategy.

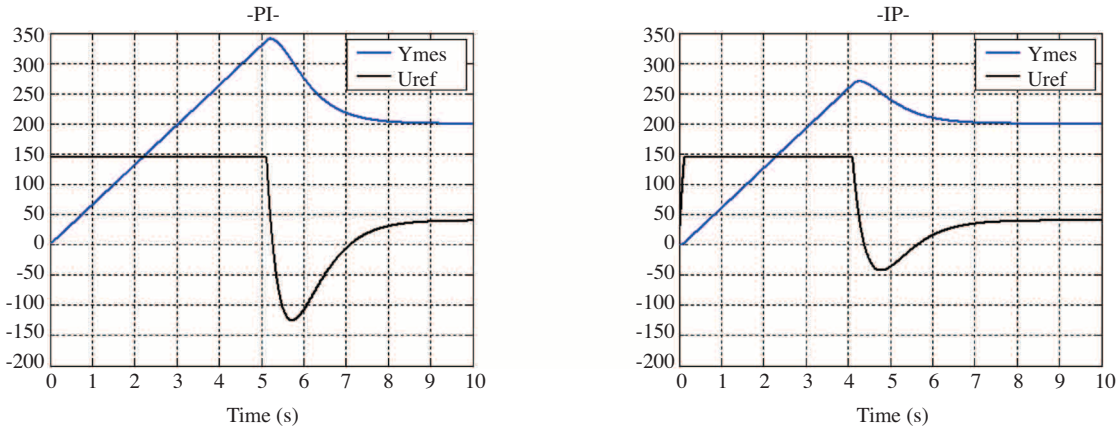

Figure 15. Phenomenon of *windup*.

5. Simulation Results

In order to characterise the electronic differential system for an electric vehicle driven by two permanent magnet synchronous motors attached to the rear wheels using direct torque fuzzy control, four different cases of simulations of the model shown Figure 16 were carried out.

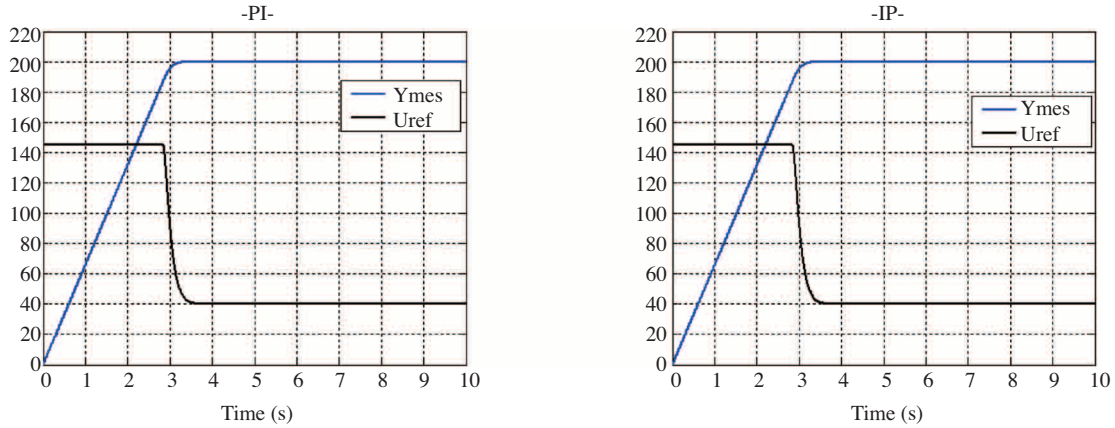

Figure 16. *Anti-windup* strategy.

Case 1: Straight road with constant speed 80 km/h

A 80 km/h speed-step is applied to our system, and in the transient state the torque is limited to 145 N·m. A good tracking of the speed step can be observed (see Figure 17(a)). The vehicle reaches constant speed at 5.33 s. Delay in reaching this speed follows from acceleration of the vehicle mass. In Figures 17(g) and 17(h), variation of phase currents for each motor is shown. Notice the presence of two general regimes. First occurs when each motor solicits a high current to attain the reference torque or speed imposed by the driver. This current arises from the demand for the accelerating torque. The second regime begins at $t = 5.33$ s, when the vehicle reaches the speed specified by the driver. At this point the motor torque reduces to a lower but steady-state value, as what would be needed and expected to maintain a constant speed. Figures 17(e)–(i) gives a comprehensive history of the above events. Figure 17(j) shows the zoomed transient and steady state currents for the right and left motors..

Case 2: Straight road with 10% slope at 80 km/h speed

This test shows the influence of the road slope on the vehicle moving on straight road. Speed of the driving wheels stay the same and the road slope does not affect the angular control of the wheels. There is only change in the motor torque, as shown in Figure 18(e). The presence of slope causes a large increase in the phase current of each motor, as shown in Figures 18(g, h). System behaviour is shown in Figures 18(a–d). The behaviour of traction is illustrated in Figure 14(f). The resistive torques are shown in Figure 18(i). Figure 18(j) shows the zoomed currents before and during the road slope for the right and left motors.

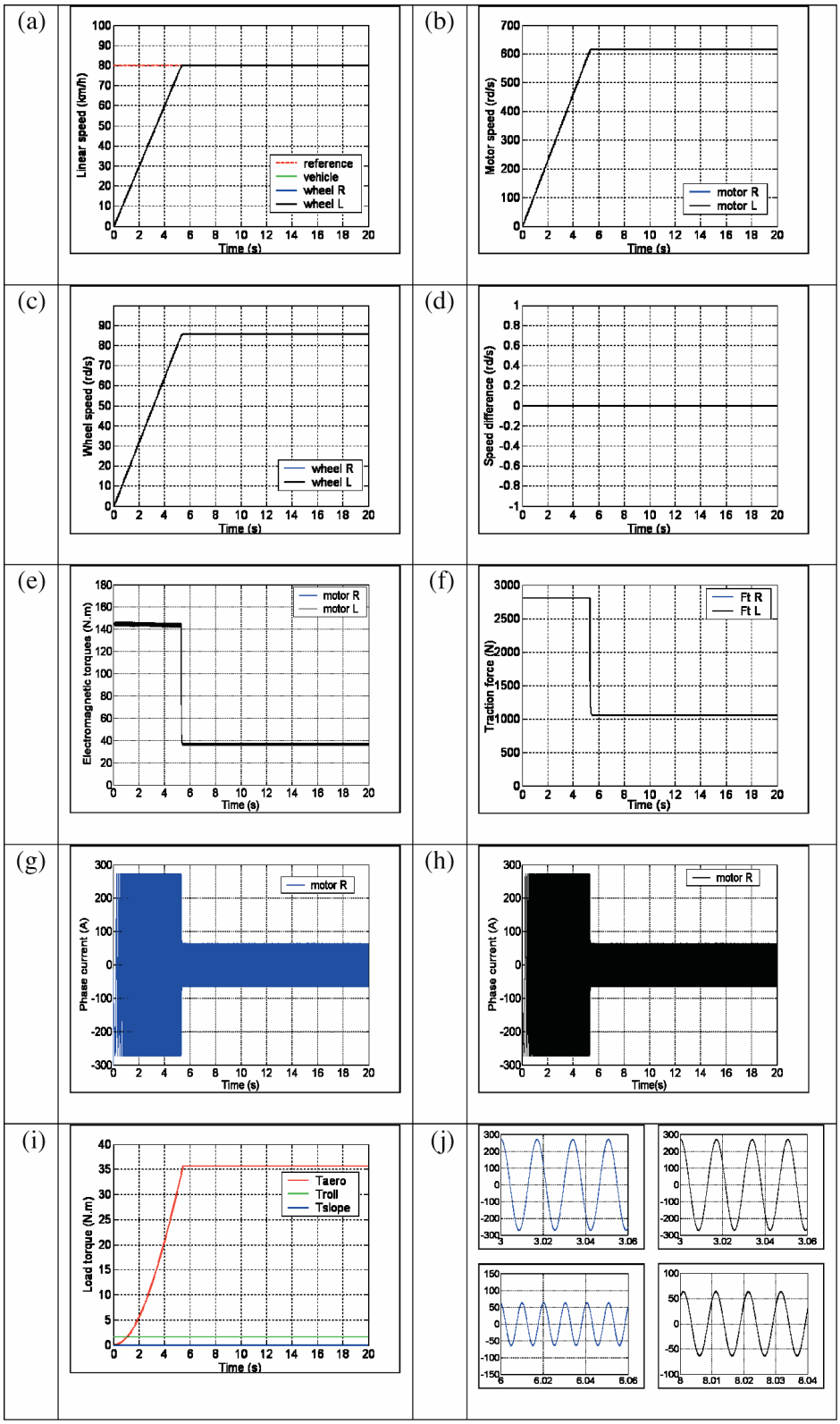

Figure 17. Results for simulation Case 1.

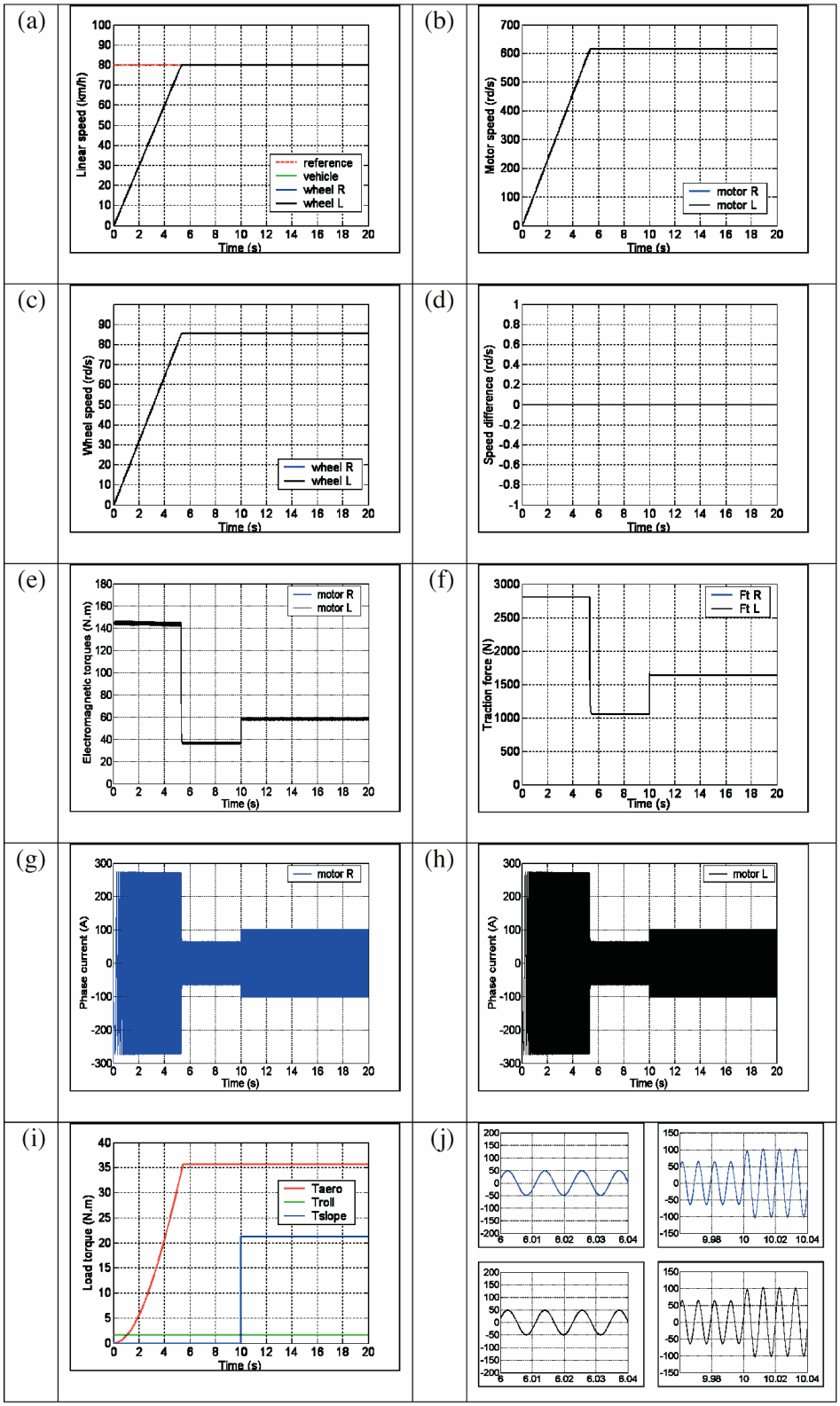

Figure 18. Results for simulation Case 2.

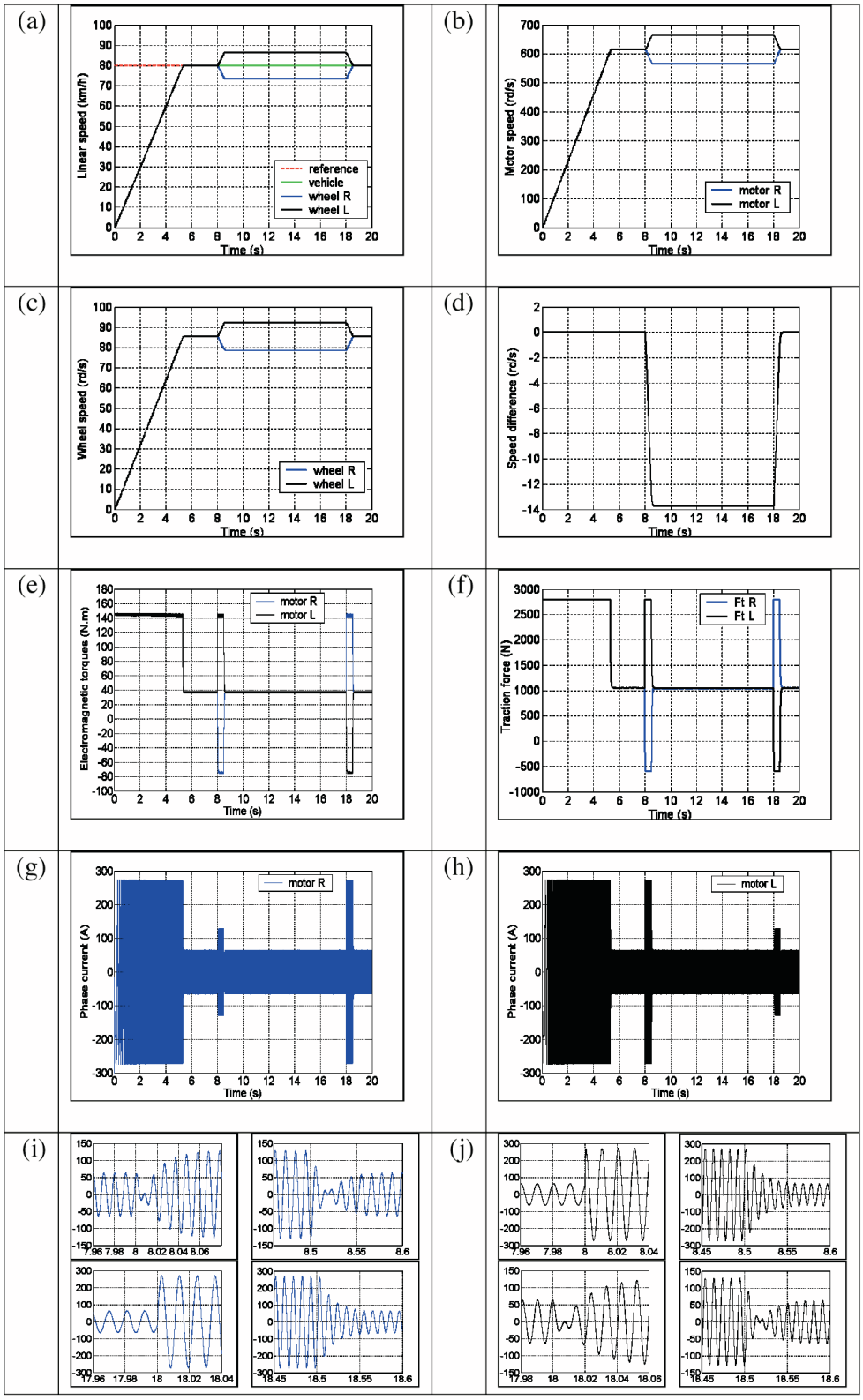

Figure 19. Results for simulation Case 3.

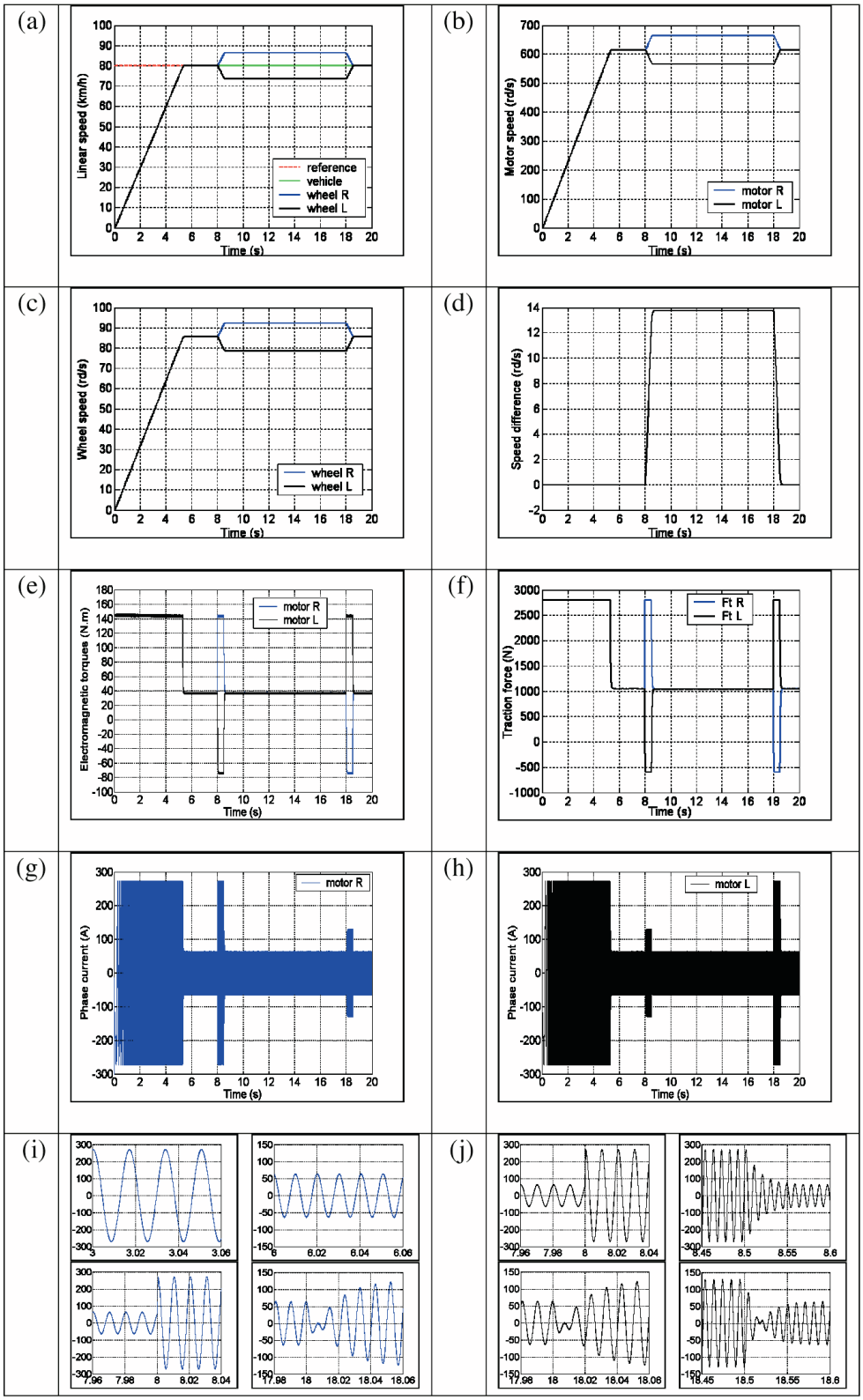

Figure 20. Results for simulation Case 4.

Case 3: Clockwise-curved road at speed 80 km/h

In this test case, the vehicle is modeled on a clockwise-curved road, accelerated with constant torque to steady speed 80 km/h. In our model, the steering angle is applied at $t = 8$ s to the front wheels. As expected, after reaching steady speed, when the vehicle enters the curved section, the speed of the right wheel decreases according to its new reference (Equation 8); in compensation, the torque of the right wheel decreases, briefly becoming negative. Negative torque is, in essence, braking mode. This working phase can be exploited for energy recuperation. Once the speed of the right wheel is stabilised, the torque returns to its initial value, as it is shown in Figure 19(c). At $t = 18$ s the vehicle exits the curved section of road; thus the driver applies an inverse steering angle to the front wheels. The electronic differential subsequently acts to equalise the speed of the drive motors; see Figure 19(d). The variation of phase currents are shown in Figures 19(g)–(j).

Case 4: Counter-clockwise-curved road at speed 80 km/h

In this case, The vehicle is moving on a curved road on the left side at a speed of 80 km/h. Despite the driving wheels follow different paths, they turn in the same direction with different speeds. The left-rear (drive) wheel turns slower through the arc than the right-rear wheel. The speed of these wheels, as a function of time, is shown in Figures 20(a), (b), (c), and (d). As the speed of the right wheel increases, the motor torque in this wheel increases and tries to compensate for change in speed. This change leads to a positive peak that corresponds to the speed of the right wheel. Once this speed stabilises, the torque returns to its initial value which corresponds to the total resistive torque applied on the motor wheels; the behaviour is shown in Figure 20(e).

6. Conclusion

This work has presented the simulation of an electric vehicle controlled by an electronic differential with two rear-wheel driven permanent magnet in-wheel synchronous motor drives. The proposed control structure, called independent machine for speed control, permits control via electronic differential. A DTFC strategy for PMSM is proposed in this study, in order to achieve good steady state and dynamic performance. Simulation results show that this structure permits an electronic differential that can ensure good static and dynamic performance. The electronic differential controls the drive wheel speeds with high accuracy on both flat and curved paths.

Abreviations

DTFC: Direct Torque Fuzzy Control

EV: Electric Vehicle

MMS: Multi-machine Multi-converter Systems

MS: Mechanical Source

PMSM: Permanent Magnet synchronous Machine

SC: Static converter

SVM: Space Vector Modulation

Parameters and Symbols

Table A1. The specifications of the vehicle used in simulation.

Vehicle total mass	1200 kg
Distance between two wheels and axes	2.5 m
Distance between the back and the front wheel	1.5 m
Wheel radius	0.26 m
Vehicle frontal area	1.9 m^2
Aerodynamic drag coefficient	0.25 $N/(ms)^2$
Gearbox ratio	7.2
Efficiency of the gearbox	98%
Battery energy capacity	25.2 kWh
Autonomy	205 km

Table A2. The specifications of motors.

Resistance	0.03 Ω
$d-$axis inductance	0.2 mH
r $q-$axis inductance	0.2 mH
Permanent magnet flux	0.08 Wb
Pole pairs	4

Symbol Nomenclature

$i_{s\alpha}, i_{s\beta}$:	$\alpha-$ and β-axis currents	ρ :	Air density
$v_{s\alpha}, v_{s\beta}$:	$\alpha-$ and β-axis voltage	S :	Front area of vehicle
v_a, v_b, v_c :	Stator voltage	C_x :	Aerodynamic coefficient
S_a, S_b, S_c :	Switching states	g :	Acceleration of gravity
R_s :	Stator resistance	μ :	Friction coefficient
L_s :	Stator inductance	α :	Angle of the slope
p :	Number of poles	v_h :	Linear speed of vehicle
θ :	Rotor position	E :	Battery voltage
ω_m :	Motor rotor speed	k_{gear} :	Report of speed gear
Φ_f :	Permanent magnet flux	M :	Vehicle mass
J :	Rotor inertia	R_r :	Wheel radius
T_{em} :	Electromgnetic torque	J_v :	Vehicle inertia
T_r :	Load torque	d_ω :	Distance between the back and the front wheel
l_ω :	Distance between two wheels and axes		

References

[1] A. Bouscaylor, B. Davat, B. de Fornel, B. Fraçois, "Multimachine Multiconverter System : application for electromechanical drives," *European Physic Journal – Applied Physics,* vol. 10, no. 2, pp. 131-147, 2000.

[2] E., Benkhoris F., "Control structures for multi-machine multi-converter systems with upstream coupling," *Elsevier, Mathematics and computers in simulation,* vol. 63, pp. 261-270, 2003.

[3] I. Takahachi and T. Noguchi, "A new quick-response and high-efficiency control strategy of an induction motor," *IEEE Trans. Ind. Applicat.,* vol. 22, no. 5, pp. 820-827, 1986.

[4] T. J. Vyncke, J. A. Melkebeek, and R. K. Boel, "Direct torque control of permanent magnet synchronous motors - an overview," *in conf.Proc. 3rd IEEE Benelux Young Research Symposium in Electrical Power Engineering,* no. 28, Ghent, Begium, Apr. 27-28, p.5, 2006.

[5] Y. Hori, senior member IEEE, "Future vehicles driver by electricity and control research on four wheel motored -UOT electric march II," *IEEE Transactions on Industrial Electronics,* vol. 51, no. 5, pp. 954 – 962, 2004.

[6] A. Bouscaylor, B. Davat, B. de Fornel, B. François, "Multimachine Multiconverter System for drives: analysis of coupling by a global modeling," *Proc. Of IEEE-IAS,* vol.3, pp.1474-1481, 2000.

[7] P. Pragasen, R. Krishnan. "Modeling, Simulation, and Analysis of Permanent Magnets Motor Drives, Part I: The Permanent Magnets Synchronous Motor Drive," *IEEE Transactions on Industry Applications.* Vol.25, no.2, 265-273, 1989.

[8] D.A.J. Rand, R. Woods, R.M. DELL. "Batteries for electric vehicles," *Research Studies.* Press Ltd. 1997.

[9] L.T. Lam, N.P. High, C.G. Phyland, A.J. Urban, Elservier, power sources, vol. 144, pp. 552-555, 2005.

[10] L.T. Lam, R. Lovey, "*Developpement of ultra-battery for hybrid-electric vehicle applications*," Elservier, power sources, vol. 158, pp. 1140-1148, 2006.

[11] S. Kandler, C.Y. Wang, "*Power and thermal characterization of Lithium-Ion battery pack for hybrid- electric vehicles*," Elservier, Power Sources, vol. 160, pp. 662-673, 2006.

[12] T. Gillespice. "Fundamentals of vehicle dynamics," *Society of Automotive Engineers*, ISBN 1-56091-199-9.

[13] Cao, Xianqing, Zang, Chunhua, Fan, Liping, "*Direct Torque Controlled Drive for Permanent Magnet Synchronous Motor Based on Neural Networks and Multi Fuzzy Controllers,* " *IEEE International Conference on* Robotics and Biomimetics, 2006. ROBIO '06. pp. 197 – 201, 2006.

[14] T. Chapuis, D. Roy, S. Courtine. "Commande directe du couple d'une machine asynchrone par le contrôle direct de son flux statorique," *Journal de physique III* n ° 6, France, Juin 1995.

[15] M. Vasudevan, R. Arumugam, "*New direct torque control scheme of induction motor for electric vehicles,* " *5th Asian* Control Conference, vol. 2, 20-23, pp. 1377 – 1383, 2004.